Z. Kristallogr. **220** (2005) 574–579

© by Oldenbourg Wissenschaftsverlag, München

First-principles codes for computational crystallography in the Quantum-ESPRESSO package

Sandro Scandolo*, [I, II], Paolo Giannozzi[I, III], Carlo Cavazzoni[IV], Stefano de Gironcoli[I, V], Alfredo Pasquarello[VI] and Stefano Baroni[I, V]

[I] INFM/Democritos National Simulation Center, 34014 Trieste, Italy
[II] The Abdus Salam International Centre for Theoretical Physics (ICTP), Strada Costiera 11, 34014 Trieste, Italy
[III] Scuola Normale Superiore, P.za dei Cavalieri 7, 56126 Pisa, Italy
[IV] Consorzio Interuniversitario per il Calcolo Automatico dell' Italia Nord Orientale (CINECA), 40033 Casalecchio di Reno, Italy
[V] International School for Advanced Studies (SISSA), Via Beirut 2–4, 34014 Trieste, Italy
[VI] Institut de Théorie des Phénomènes Physiques (ITP), Ecole Polytechnique Fédérale de Lausanne (EPFL), 1015 Lausanne, Switzerland and Institut Romand de Recherche Numérique en Physique des Matériaux (IRRMA), 1015 Lausanne, Switzerland

Received August 6, 2004; accepted December 5, 2004

Ab-initio calculations / Molecular dynamics / Phonons / Elasic constants / High-pressure / Quantum-ESPRESSO Computer program / Computational crystallography

Abstract. The Quantum-ESPRESSO package is a multi-purpose and multi-platform software for *ab-initio* calculations of condensed matter (periodic and disordered) systems. Codes in the package are based on density functional theory and on a plane wave/pseudopotential description of the electronic ground state and are ideally suited for structural optimizations (both at zero and at finite temperature), linear response calculations (phonons, elastic constants, dielectric and Raman tensors, etc.) and high-temperature molecular dynamics. Examples of applications of the codes included in the package are briefly discussed.

Introduction

With the support of the *Democritos* National Simulation Center (http://www.democritos.it), a number of codes for first-principles electronic structure calculations have been merged into a single multi-purpose and multi-platform package, called Quantum-ESPRESSO (standing for Quantum-*opEn-Source Package for Research in Electronic Structure, Simulation, and Optimization*). The package is freely distributed under the GNU open source license at the Democritos web site. The three main components of the package are:

- PWscf (Plane Wave self-consistent field), developed by S. Baroni, S. de Gironcoli, A. Dal Corso, P. Giannozzi and others (Baroni, de Gironcoli, Dal Corso, Giannozzi, 2001);
- CP (Car-Parrinello), developed by A. Pasquarello, K. Laasonen, A. Trave, R. Car, P. Giannozzi, N. Marzari and others (Pasquarello et al., 1992; Laasonen et al., 1993; Giannozzi, de Angelis, Car, 2004);
- FPMD (First-Principles Molecular Dynamics), developed by C. Cavazzoni, S. Scandolo, G. Chiarotti, P. Focher, G. Ballabio and others (Focher et al., 1994; Cavazzoni and Chiarotti, 1999).

While the three original components can still be used separately, they are now integrated into a single framework for input and output data and share the installation mechanism and a large common code basis. The package uses plane wave basis sets for the expansion of the electronic wave function, a pseudopotential description of the electron-ion interaction (Pickett, 1989), and density functional theory (DFT) (see e.g. Dreizler and Gross, 1990) for the description of electron-electron interactions. The package can calculate the ground-state energy and Kohn-Sham orbitals for both insulators and metals, in any crystal structure, for many exchange-correlation functionals. It can perform various types of structural optimizations and of variable-cell molecular dynamics, both Car-Parrinello and with electrons on their ground state (Marx and Hutter, 2000). The Nudged Elastic Band method for the estimation of energy barriers is also implemented. Spin polarization, noncolinear magnetism, and spin-orbit coupling can be accounted for.

Energy derivatives and related quantities are analytically calculated using Density-Functional Perturbation Theory (DFPT) (Baroni, de Gironcoli, Dal Corso, Giannozzi, 2001). The list of implemented features includes the calculation of phonon frequencies and eigenvectors at a generic wave vector, effective charges and dielectric tensors, interatomic force constants in real space, electron-phonon interaction coefficients for metals, third-order anharmonic phonon lifetimes, non resonant Raman scattering coefficients. Finally, a nonperturbative calculation of the macroscopic polarization via the Berry Phase is available.

The package works on many different types of machines, including parallel machines. For the latter case, highly scalable parallel algorithms using the Message-Passing Inter-

* Correspondence author (e-mail: scandolo@ictp.trieste.it)

face (MPI) library are implemented. The package includes a Graphical User Interface (GUI), based on the GUIB library developed by Anton Kokalj (http://www-k3.ijs.si/kokalj/guib/), that facilitates the production of input data files. Various auxiliary codes for postprocessing of output data are available, producing data in formats that can be directly visualized by several graphical packages. We mention in particular the interface with the XCrySDen graphical plotting program (Kokalj, 2003), available from http://www.xcrysden.org). Auxiliary codes for pseudopotential generation are also included in the distribution.

The package is available for download from: http://www.democritos.it/scientific.php

The three codes have been extensively used to address crystallography-related problems. In the following we pick up examples of applications for each of them. We stress that differences at the user's level between codes are presently minimal and will eventually disappear. For example, differences between the CP and the FPMD codes are presently restricted to the possibility to work with ultrasoft pseudopotentials (which is active in CP but not in FPMD), and by a better optimization of the constant-pressure molecular dynamics feature in FPMD. Such differences will be removed shortly.

PWscf

An important feature of PWscf is the possibility to calculate the entire phonon dispersions, at any wave vector, for relatively complex materials (up to several tens of atoms). Phonon dispersions play an important role in both pressure-induced and temperature-induced phase transitions. Their knowledge at the DFT level is of considerable help in the study of crystal stability.

An example of systems in which pressure-induced phase transitions are driven by phonons is provided by Cs halides. In these materials, a cubic-to-orthorhombic transition, driven by the softening of an acoustic phonon at the M point of the Brillouin zone, is competing with the cubic-to-tetragonal martensitic transition typical of these compounds. The phonon softening takes place only in CsI (see Fig. 1) and CsBr, when the volume V is respectively

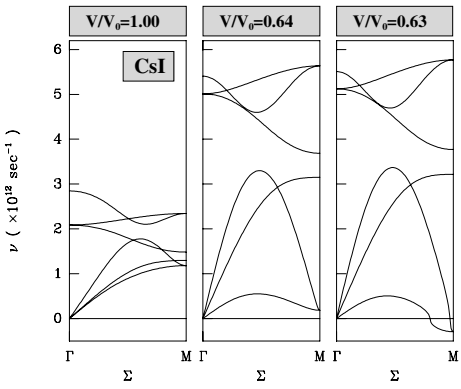

Fig. 1. Phonon dispersion along the (110) Σ direction for CsI at equilibrium volume and just above and below the softening pressure of the M_5^- acoustic mode. 'Negative' frequencies actually mean 'imaginary' (i.e. negative squared frequencies).

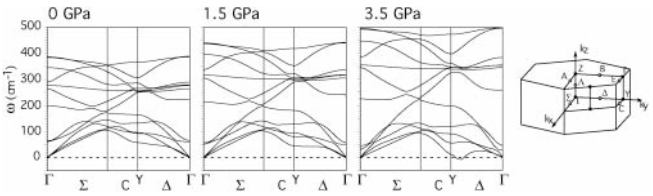

Fig. 2. Phonon dispersions in ice XI at 0, 1.5, and 3.5 GPa.

64% and 52% of the volume V_0 at zero pressure. A cubic-to-tetragonal instability is found instead to occur at $V/V_0 \approx 0.54$ for all the compounds considered here. The orthorhombic phase is stable only in CsI, whereas it is taken over by the tetragonal one in the case of CsBr. The phase transition can be analyzed using a Landau phenomenological free energy expression whose parameters are extracted from first-principles calculations. Such analysis reveals the essential role played by the phonon-strain coupling in stabilizing the orthorhombic phase and in making the corresponding transition first-order (Buongiorno Nardelli, Baroni, Giannozzi, 1995).

Further applications of phonon calculations to structural phase transitions are reported in the literature. For a review, see Baroni, de Gironcoli, Dal Corso, Giannozzi, 2001. We quote in particular a recent application to pressure-induced amorphization, a ubiquitous phenomenon observed in quartz, ice, and many other materials. In ice XI, the observed phenomenology is believed to be connected to the softening of a phonon at an incommensurate wavevector. Fig. 2 shows the phonon dispersions in ice XI at 0, 1.5, and 3.5 GPa (Umemoto et al 2004). An instability develops at $\mathbf{q} \simeq (0, {}^4/_5, 0)$ at about 3.5 GPa, followed by the collapse of the entire acoustic branch and by the violation of the Born stability criteria.

As a second example of geophysical relevance we mention recent first-principles evaluation of pressure and temperature dependence of the elastic constants and sound velocities in the major candidate phases of Earth lower mantle: MgO and $MgSiO_3$ perovskite (Karki et al., 1999; Wentzcovitch et al., 2004).

The crystal free energy were obtained within the quasi-harmonic approximation adding to the static DFT energy the vibrational contribution obtained from full phonon dispersions, computed within DFPT. The isothermal elastic constants, c_{ij}^T, of MgO (Karki et al., 1999) and $MgSiO_3$ (Wentzcovitch et al., 2004) were computed from the free energy dependence on all independent strains in the two cases and then converted to adiabatic ones c_{ij}^S, via standard thermodynamical relations: $c_{ij}^S(P,T) = c_{ij}^T(P,T) + VT\lambda_i\lambda_j/C_V$, where $\lambda_i(P,T) = [\partial S(P,T)/\partial\varepsilon_i]_P$, the ε_i's are the strains, C_V is the constant-volume specific heat, and S the entropy.

Figure 3 displays the resulting bulk (K_S) and shear (G) moduli for two isotropic and homogeneous mineralogical models along a standard adiabatic geotherm (Brown and Shankland, 1981), together with data from Preliminary Reference Earth Model (PREM) (Dziewonski and Anderson, 1981). For more details on the calculations and on the analysis of the results we refer to the original work (Karki et al., 1999; Wentzcovitch et al., 2004). The major difference between the two mineralogical models is the overall smaller *pyrolitic* K_S which agrees reasonably well with

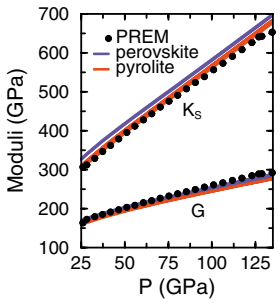

Fig. 3. Bulk (K_S) and shear (G) moduli for two isotropic and homogeneous mineralogical models along a standard adiabatic geotherm (Brown and Shankland, 1981).

K_S^{PREM} in the upper part of the lower mantle (down to $\approx$1,400 km depth or 55 GPa). Both models describe G^{PREM} reasonably well in the upper lower mantle. However with increasing depth K_S^{PREM} and G^{PREM} depart consistently and in opposite directions from the values predicted along this adiabatic geotherm. These systematic deviations toward the deep lower mantle cannot be accounted by alterations in the geotherm alone and suggest that deep and shallow lower mantle differ somehow.

CP

The code CP is particularly useful for studying the structure of disordered materials. For the purpose of illustration, we here describe an application to vitreous silica. First, we generated a disordered model structure by first-principles molecular dynamics. Then, we examined the resulting model by comparing the calculated static structure factor with the corresponding experimental result obtained by neutron diffraction.

We used the feature of the CP code for carrying out first-principles molecular dynamics using ultrasoft pseudopotentials (Pasquarello et al., 1992; Laasonen et al., 1993). Their use, in conjunction to effective algorithms, allows a considerable reduction of the computer requirements of a simulation with respect to conventional (norm-conserving) pseudopotentials. We modelled liquid SiO_2 using a periodic cubic cell with $N = 72$ atoms at a density of 2.1 g/cm^3 (Sarnthein, Pasquarello, Car, 1995a; Sarnthein, Pasquarello, Car, 1995b). We started the simulation from a configuration generated by Monte-Carlo using classical interaction potentials. The system was allowed to evolve at temperatures ranging between 2500 and 3500 K for 6 ps. In order to observe liquid-like diffusive motion, we fixed the temperature at 3500 K, and continued the evolution for other 8 ps. A model structure of vitreous silica was then obtained by quenching the temperature. The temperature was first set to 3000 K for 3 ps, and finally quenched to 300 K.

The resulting model structure consists of a chemically ordered network of corner-sharing tetrahedra. For a more extended analysis of the structural properties of this model, we refer to the work of Sarnthein, Pasquarello, and Car (1995b) for parameters such as bond lengths and angles, and to the work of Pasquarello and Car (1998) for a description in terms of ring statistics.

In order to calculate the structure factor of this model structure, a first-principles molecular dynamics was carried out at 300 K for a time period of 3 ps, during which the atoms oscillate around their equilibrium positions. The static neutron structure factor $S(\mathbf{Q})$ is calculated from the ionic positions $\mathbf{R}_I$ using the following expression:

$$S(\mathbf{Q}) = \frac{1}{\sum_I b_I^2} \left\langle \sum_{IJ} b_I b_J \, \mathrm{e}^{-i\mathbf{Q}(\mathbf{R}_I - \mathbf{R}_J)} \right\rangle , \qquad (1)$$

where the brackets $\langle \ldots \rangle$ indicate a thermal average, and the b_I are the neutron scattering lengths ($b_{\mathrm{Si}} = 4.149$ fm and $b_{\mathrm{O}} = 5.803$ fm). The calculation of $S(\mathbf{Q})$ is only performed for a discrete set of $\mathbf{Q}$ vectors, which are compatible with the periodicity of the simulation cell, and the result therefore corresponds to the infinitely repeated model (Massobrio, Pasquarello, Car, 2001). For isotropic systems, $S(\mathbf{Q})$ only depends on the modulus of $\mathbf{Q}$, and $S(Q)$ is obtained by a spherical average (Price and Pasquarello, 1999). The thermal average is obtained by considering the structural configurations visited during the course of the dynamics. Note, that the average obtained in this way corresponds to a classical treatment of the ionic vibrations. Figure 4a shows the comparison between the calculated structure factor and the one obtained by neutron diffraction (Susman et al., 1991). Despite the limited statistical description, the agreement is very satisfactory. In particular, the model not only accurately reproduces the short-range structure ($Q > 2$ Å^{-1}), but also accounts for the intermediate-range order manifested by the peak at $\sim$1.6 Å^{-1}.

The model considered here has also proved very successful in a series of investigations involving the vibrational properties. These properties can be accessed by using the feature of the code CP for calculating the atomic forces at fixed ionic positions. Sarnthein, Pasquarello, and Car (1997) calculated the dynamical matrix for this model

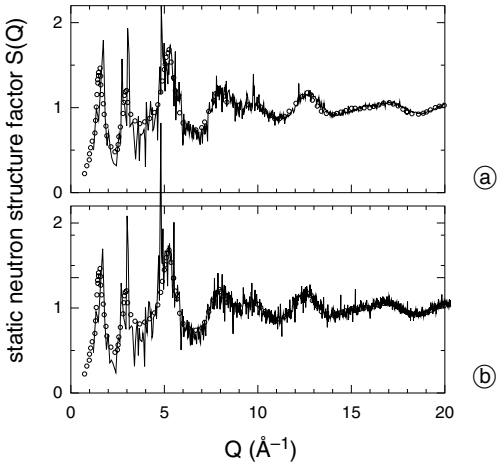

Fig. 4. Static neutron structure factor $S(Q)$ at 300 K for a model structure of vitreous silica generated with the code CP, as obtained (**a**) from a temporal average of the classical ionic motion in a first-principles molecular dynamics (Sarnthein, Pasquarello, Car, 1995a; Sarnthein, Pasquarello, Car, 1995b) and (**b**) from a quantum-mechanical treatment of the vibrations in the harmonic approximation (Pasquarello, 2000). The calculated structure factors are compared with the experimental one (circles) obtained by neutron diffraction (Susman et al., 1991).

structure by taking finite differences of the atomic forces. The vibrational frequencies ω_n and their corresponding eigenmodes $\mathbf{e}_i^n$ could then be derived by diagonalization. Vibrational properties which have been investigated are the neutron vibrational density of states (Sarnthein, Pasquarello, Car, 1997; Pasquarello, Sarnthein, Car, 1998), the infrared spectrum (Pasquarello, Car, 1997), the dynamical structure factor (Pasquarello, Sarnthein, Car, 1998), the vibrational amplitudes (Pasquarello, 2000), and the Raman spectrum (Pasquarello, Car, 1998; Umari, Gonze, Pasquarello, 2003).

We also considered an alternative approach for calculating the static neutron structure factor, which relies on the knowledge of the vibrational properties in the harmonic approximation. This alternative approach allows us to treat the ionic vibrations at the quantum-mechanical level, but misses any effect related to the anharmonicity of the vibrations. Adopting this approximation, we express the structure factor as (Pasquarello, 2000):

$$S(\mathbf{Q}) = \frac{1}{\sum_I b_I^2} \sum_{IJ} b_I b_J \, \mathrm{e}^{-W_{IJ}}(\mathbf{Q}) \, \mathrm{e}^{-i\mathbf{Q}(\bar{\mathbf{R}}_I - \bar{\mathbf{R}}_J)} \,, \qquad (2)$$

where the exponent in the Debye-Waller factor is given by

$$W_{IJ}(\mathbf{Q}) = \tfrac{1}{2} \langle [\mathbf{Q}(\mathbf{u}_I - \mathbf{u}_J)]^2 \rangle \,, \qquad (3)$$

the $\mathbf{u}_I$ being the atomic displacements with respect to the equilibrium sites $\bar{\mathbf{R}}_I$. The thermal averages indicated by $\langle \ldots \rangle$ can be expressed in terms of the vibrational frequencies ω_n and their corresponding modes $\mathbf{e}_i^n$:

$$\langle u_{I\alpha} u_{J\beta} \rangle = \sum_n \frac{\hbar}{\omega_n} \frac{e_{I\alpha}^n}{\sqrt{M_I}} \frac{e_{J\beta}^n}{\sqrt{M_J}} \left[n(\hbar\omega_n) + \frac{1}{2} \right] , \qquad (4)$$

where the temperature dependence enters through the Boson occupation number $n(E) = [\exp(E/k_B T) - 1]^{-1}$, M_I are the masses of the involved atoms, n enumerates the vibrational states, and α and β run over the Cartesian directions. The resulting structure factor for the same model structure discussed above is shown in Fig. 4b, where it can be compared with corresponding result of Fig. 4a, in which the vibrations were treated classically, as well as with the experimental result of Susman et al. (1991). Overall, the differences between the two simulated structure factors are minor. A more extended analysis of the structure factor as a function of temperature is given by Pasquarello (2000).

FPMD

One of the most attractive features of the FPMD code is the capability of carrying out molecular dynamics simulations in the constant-pressure ensemble, by means of a variable cell algorithm originally developed for classical molecular dynamics by Parrinello and Rahman (1980) and subsequently implemented in the FPMD code (Bernasconi et al., 1995). The algorithm allows the volume and shape of the simulation box to change dynamically. The dynamics of the box parameters are controlled by the unbalance between the imposed pressure and the instantaneously calculated value of the stress tensor. At equilibrium the shape and volume of the box is such that the internal stress coincides with the external pressure. The algorithm can thus be used for the optimization of structural and crystal parameters. During a molecular dynamics run at finite temperature, however, the box parameters can either fluctuate dynamically around the equilibrium position if this is a stable minimum of the free energy, or can undergo changes and spontaneously search for a lower minimum in the case of a pressure-induced phase transformation.

The power of the variable-cell method is illustrated here with two examples.

The first example deals with the prediction of a pressure-induced first-order phase transition in carbon dioxide (CO_2) from the molecular phase stable at ambient conditions into a non-molecular phase at high pressure (Serra et al., 1999). The simulation started with carbon dioxide in the molecular phase β-CO_2 (Fig. 5a) with *Cmca* space group. The validity of the computational scheme was initially checked by comparing our optimized β-CO_2 molecular lattice structure with the X-ray data at 12 GPa and finding that errors were smaller than 0.3%. Moreover, the tilt angle of the molecules relative to the c axis, usually difficult to reproduce because of its weak energy dependence, was calculated to be 52.5°, consistent with the experimental value of 52°. Temperature was then raised to 1000 K and pressure slowly increased at small increments up to 100 GPa, where β-CO_2 transformed spontaneously into the layered non-molecular phase, shown in Fig. 5b. The new structure consisted of carbon-centered oxygen tetrahedra, similar to Si-centered tetrahedra in silica, arranged in a two-dimensional tetragonal layered structure of space group $P42/nmc$ and two CO_2 units per cell (Fig. 5b). Subsequent simulations by us and by other groups have continued to support the notion that pressure induces formation of well-defined CO_4 tetrahedra-based solids, and experiments have confirmed this picture (Iota and Yoo, 2001). The exact structure of high-pressure CO_2 is still a matter of controversy however.

The second example, compressed liquid hydrogen, illustrates the capability of the method to describe structural transformations induced by pressure in liquids. The search for a metallic state and the abundance of hydrogen in stars and giant planets have stimulated widespread interest in the states of hydrogen at extreme conditions of pressure and

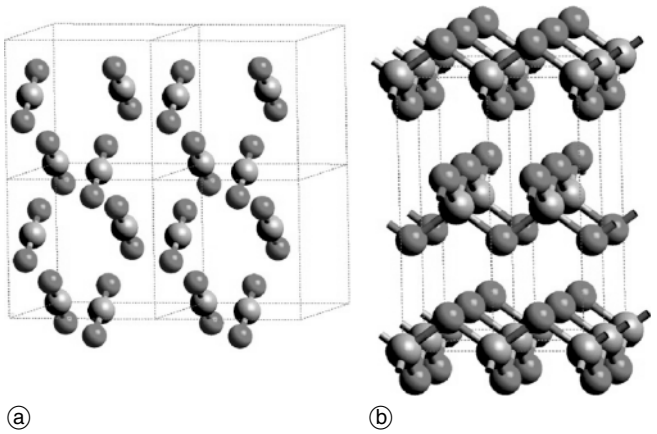

Fig. 5. Crystal structure of the high-pressure molecular phase β-CO_2 (**a**) and of the extended layered structure of space group $P42/nmc$ found in the simulation (**b**).

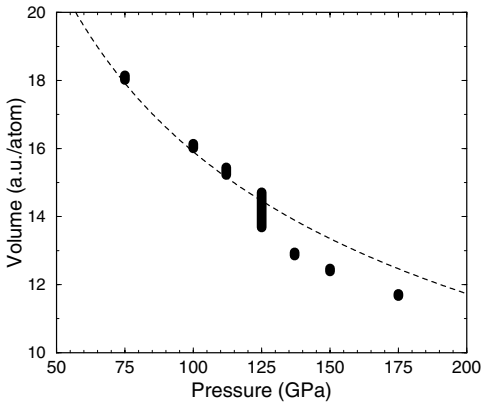

Fig. 6. Average volume calculated in a first-principles molecular dynamics simulation of hydrogen at 1500 K. The phase transition at 125 GPa involves a change of the atomic structure from molecular to non molecular (Scandolo, 2003).

temperature (Oganov, Price, and Scandolo, 2005). Extrapolations of the experimentally determined freezing line suggest that the freezing temperature could cease to increase after reaching 1100 K at a critical pressure of about 120 GPa (Datchi, Loubeyre, LeToullec, 2000). A sign reversal of the freezing slope implies, through the Clausius-Clapeyron relation, that the liquid becomes denser than the solid above 120 GPa. This raises fundamental questions about the structure of the compressed liquid, and in particular about the extent of its structural differences with respect to the molecular solid. Simulations with cells containing 448 atoms were performed with the Car-Parrinello method and the variable-cell algorithm at 1500 K and pressures from 75 to 175 GPa (Scandolo, 2003). Protons were assumed to behave as classical particles. This is a good approximation at 1500 K, because quantum effects on the the ground state structure are roughly equivalent to classical thermal effects at 500 K in the classical system (Biermann, Hohl, Marx, 1998). The system persisted in a molecular state from 75 GPa to about 125 GPa, at which pressure the cell displayed an abrupt volume change of about $6(\pm 2)\%$, corresponding to the loss of the molecular character (Fig. 6).

The transition appears to be first-order in the simulation, and may have important implications for our understanding of the giant planets Jupiter and Saturn, which are mostly composed of hydrogen (Oganov, Price, and Scandolo, 2005).

Outlook

The development of the Quantum-ESPRESSO package will continue towards a more seamless integration of the three packages (presently still incomplete), to be achieved via a better structured, more modular code. The inclusion of new features, in particular exciting recent developments such as Time-Dependent DFT, is of course planned. Better documentation for both users and developers willing to contribute new features will be needed. Finally, at least some form of interoperability with other codes for electronic structure calculation and with graphical and analysis tools will be pursued. This means in practice that some form of standard format for both data exchange and output results should be agreed on and adopted.

Acknowledgments. A special thank goes to all the members of the "Democritos" Center for their precious help in developing, maintaining, and distributing the package. In particular, we wish to thank G. Deinzer, S. Fabris, A. Mosca Conte, M. Profeta, and C. Sbraccia.

Codes contained in the Quantum-ESPRESSO package are the result of many years of development of a countless number of researchers. We wish to thank all of them for their contribution as well as for their availability to make their work publicly available through the package.

References

Baroni, S.; de Gironcoli, S.; Dal Corso, A.; Giannozzi, P.: Phonons and related crystal properties from density-functional perturbation theory. Rev. Mod. Phys. **73** (2001) 515–562.

Bernasconi M.; Chiarotti G. L.; Focher P.; Scandolo, S.; Tosatti E.; Parrinello M.: First-principle constant pressure molecular dynamics. J. Phys. Chem. Solids **56** (1995) 501.

Biermann, S.; Hohl, D.; Marx, D.: Quantum effects in solid hydrogen at ultra-high pressure. Sol. St. Commun. **108** (1998), 337–341.

Brown, J. M.; Shankland, T. J.: Thermodynamic parameters in the Earth as determined from seismic profiles. Geophys. J. R. Astr. Soc. **66** (1981) 579–596.

Buongiorno Nardelli, M.; Baroni, S.; Giannozzi, P.: High-Pressure Low-Symmetry Phases of Cesium Halides. Phys. Rev. B**51** (1995) 8060–8068.

Cavazzoni, C.; Chiarotti, G. L.: A parallel and modular deformable cell Car-Parrinello code. Computer Phys. Commun. **123** (1999) 56–76.

Datchi, F.; Loubeyre, P.; LeToullec, R.: Extended and accurate determination of the melting curves of argon, helium, ice (H_2O) and hydrogen (H_2). Phys. Rev. B**61** (2000) 6535–6546.

Dziewonski, A. D.; Anderson, D. L.: Preliminary reference Earth model. Phys. Earth Planet. Int. **25** (1981) 297.

Dreizler, R. M.; Gross, E. K. U.: Density Functional Theory. Springer-Verlag, Berlin (1990).

Focher, P.; Chiarotti, G. L.; Bernasconi, M.; Tosatti, E.; Parrinello, M.: Structural phase-transformations via first-principles simulation. Europhys. Lett. **26** (1994) 345–351.

Giannozzi, P.; de Angelis, F.; Car, R.: First-principle molecular dynamics with ultrasoft pseudopotential: parallel implementation and application to extended bioinorganic systems. J. Chem. Phys. **120** (2004) 5903–5915.

Iota, V.; Yoo C. S.: Carbon dioxide at high pressure and temperature. Phys. Status Solidi B**223** (2001) 427–433.

Karki, B. B.; Wentzcovitch, R. M.; de Gironcoli, S.; Baroni, S.: First-Principles Determination of Elastic Anisotropy and Wave Velocities of MgO at Lower Mantle Conditions. Science **286** (1999) 1705.

Kokalj, A.: Computer graphics and graphical user interfaces as tools in simulations of matter at the atomic scale. Computational Materials Science **28** (2003) 155–168.

Laasonen, K.; Pasquarello, A.; Car, R.; Lee, C.; Vanderbilt, D.: Car-Parrinello molecular dynamics with Vanderbilt ultrasoft pseudopotentials. Phys. Rev. B**47** (1993) 10142–10150.

Massobrio, C.; Pasquarello, A; Car, R.: Short- and intermediate-range structure of liquid $GeSe_2$. Phys. Rev. B**64** (2001) 144205.

Marx, D.; Hutter, J.: Ab initio molecular dynamics: theory and implementation. In: *Modern Methods and Algorithms of Quantum Chemistry*, pp. 301–449. John von Neumann Institute for Computing, FZ Jülich, 2000.

Oganov, A. R.; Price, G. D.; Scandolo S.: *Ab initio* theory of planetary materials. Z. Kristallogr. **220** (2005) 531–548.

Parrinello, P.; Rahman A.: Crystal structure and pair potentials: a molecular-dynamics study. Phys. Rev. Lett. **45** (1980) 1196–1199.

Pasquarello, A.; Laasonen, K.; Car, R.; Lee, C.; Vanderbilt, D.: *Ab initio* molecular dynamics for *d*-electron systems: Liquid copper at 1500 K. Phys. Rev. Lett. **69** (1992) 1982–1985.

Pasquarello, A.; Car, R.: Dynamical charge tensors and infrared spectrum of amorphous SiO_2. Phys. Rev. Lett. **79** (1997) 1766–1769.

Pasquarello, A.; Sarnthein, J.; Car, R.: Dynamic structure factor of vitreous silica from first principles: Comparison to neutron-inelastic-scattering experiments. Phys. Rev. B**57** (1998) 14133–14140.

Pasquarello, A.; Car, R.: Identification of Raman defect lines as signatures of ring structures in vitreous silica. Phys. Rev. Lett. **80** (1998) 5154–5156.

Pasquarello, A.: Vibrational amplitudes in vitreous silica. Phys. Rev. B**61** (2000) 3951–3959.

Pickett, W. E.: Pseudopotential method in condensed matter physics. Computer Phys. Reports **9** (1989) 115–196.

Price, D. L.; Pasquarello, A.: Number of independent partial structure factors for a disordered *n*-component system. Phys. Rev. B**59** (1999) 5–7.

Sarnthein, J.; Pasquarello, A.; Car, R.: Structural and electronic properties of liquid and amorphous SiO_2: An *ab initio* molecular dynamics study. Phys. Rev. Lett. **74** (1995a) 4682–4685.

Sarnthein, J.; Pasquarello, A.; Car, R.: Model of vitreous SiO_2 generated by an *ab initio* molecular dynamics quench from the melt. Phys. Rev. B**52** (1995b) 12690–12695.

Sarnthein, J.; Pasquarello, A.; Car, R.: Origin of the high-frequency doublet in the vibrational spectrum of vitreous SiO_2. Science **275** (1997) 1925–1927.

Scandolo, S.: Liquid-liquid phase transition in compressed hydrogen from first-principles simulations. Proc. Natl. Acad. Sci. USA **100** (2003) 3051–3053.

Serra, S.; Cavazzoni, C.; Chiarotti, G. L.; Scandolo, S.; Tosatti, E.: Pressure-induced solid carbonates from molecular CO_2 by computer simulation. Science **284** (1999) 788–790.

Susman, S.; Volin, K. J.; Price, D. L.; Grimsditch, M.; Rino J. P.; Kalia R. K.; Vashishta, P.; Gwanmesia, G.; Wang, Y.; Liebermann, R. C.: Intermediate-range order in permanently densified vitreous SiO_2 – a neutron-diffraction and molecular-dynamics study. Phys. Rev. B**43** (1991) 1194–1197.

Umari, P.; Gonze, X.; Pasquarello, A.: Concentration of small ring structures in vitreous silica from a first-principles analysis of the Raman spectrum. Phys. Rev. Lett. **90** (2003) 027401.

Umemoto, K.; Wentzcovitch, R. M.; Baroni, S.; de Gironcoli, S.: Anomalous pressure-induced transition(s) in Ice XI. Phys. Rev. Lett. **92** (2004) 105502.

Wentzcovitch, R. M.; Karki, B. B.; Cococcioni, M.; de Gironcoli, S.: Thermoelastic Properties of $MgSiO_3$-Perovskite: Insights on the Nature of the Earth's Lower Mantle. Phys. Rev. Letters **92** (2004) 018501.